

Kremer-Grest models for commodity polymer melts: Linking theory, experiment and simulation at the Kuhn scale

Carsten Svaneborg,^{1,*} Hossein Ali Karimi-Varzaneh,² Nils Hojdis,² Frank Fleck,² and Ralf Everaers³

¹*University of Southern Denmark, Campusvej 55, DK-5230 Odense M, Denmark*

²*Continental, PO Box 169, D-30001 Hannover, Germany*

³*Université de Lyon, ENS de Lyon, UCBL, CNRS, Laboratoire de Physique and Centre Blaise Pascal, Lyon, France*

The Kremer-Grest (KG) polymer model is a standard model for studying generic polymer properties in Molecular Dynamics simulations. It owes its popularity to its simplicity and computational efficiency, rather than its ability to represent specific polymers species and conditions. Here we show, that by tuning the chain stiffness it is possible to adapt the KG model to model specific real polymers. In particular, we provide mapping relations from KG to SI units for a wide range of commodity polymer melts. The connection between the experimental and the KG melts is made at the Kuhn scale, i.e. at the crossover from chemistry-specific small scale to the universal large scale behavior. Nevertheless, we expect the KG models to faithfully represent universal properties dominated by the large scale conformational statistics and dynamics of flexible polymers. As an example, we compare entanglement moduli to experimental data for the target systems.

PACS numbers:

I. INTRODUCTION

Polymers are long chain molecules built by covalent linkage of a large numbers of identical monomers [1, 2]. Some properties of polymeric materials such as their density or glass transition temperature depend on chemical details at the monomer scale. Others, like the variation of the melt viscosity with the molecular weight of the chains, are controlled by the large scale conformational statistics and dynamics of long entangled chains adopting interpenetrating random walk conformations [3]. These latter properties, which are characteristic of polymeric systems, are universal [4, 5] in the sense that a large number of chemically different systems show the same behavior, if expressed in suitable material-specific units.

The character of the target properties is crucial for the choice of a model in theoretical or computational investigations. Universal properties can be studied using simple, analytically or numerically convenient lattice and off-lattice models, see e.g. refs. [3, 6–8] for reviews. In contrast, predicting specific materials properties for a given chemical species often requires atom-scale modeling [9]. A growing body of work aims at developing such coarse-grained (CG) polymer models [10–14] designed for specific polymer chemistries such as polyethylene [15–17], polyisoprene [18–21], polystyrene [22–24], polyamide [25, 26], polymethacrylate [27], polydimethylsiloxane [21], bisphenol-A polycarbonate [28–30], polybutadiene [31], polyvinyl [32], and polyisobutylene [21].

Common to these approaches is the selected inclusion of specific chemical details in the coarse-grained models. They offer insights into which atomistic details of the chemical structure are relevant for partic-

ular non-universal polymer properties. The preservation of relevant molecular details is supposed to preserve a certain degree of transferability, i.e. models optimized to describe materials at one state point are expected to remain approximately valid at neighboring state points. [13, 33, 34] Similarly, careful coarse-graining is supposed to assure representability, i.e. the ability of a model to predict properties that it was not explicitly designed to reproduce. [35]

In the present paper, we use a minimal route to include specificity into a generic polymer model, where non-trivial large scale features *emerge* through the same mechanisms as in the experimental target systems. With universality assuring the strongest form of representability, we expect that by matching a very limited number of conformational properties [36], we can 1) design generic polymer models that match universal properties of real chemical polymers, and 2) map simulation results for such models to real units and hence make quantitative predictions for target systems. Without needing to be accurate on the atomic scale, such models can properly account for entanglement effects including multichain mechanism such as constraint release [37–41], the formation of correlation holes [42], chain structure [43] and polydispersity [44], branching [45], chemical cross-linking [46–48], network aging [49], the generic effects of spatial confinement [50], in thin films [51], due to grafting [52–54] or the addition of filler particles in composite materials [55, 56], as well as the welding dynamics at polymer interfaces [57, 58]

Here we apply this philosophy to the most popular Molecular Dynamics polymer model introduced by Kremer and Grest (KG) [59, 60]. In the KG model approximately hard sphere beads are connected by strong non-linear springs generating the connectivity and the liquid-like monomer packing characteristic of polymer melts. The spring potential is chosen to energetically prevent

*Electronic address: science@zqex.dk

two polymer chains from passing through each other and thus to assure that the model reproduces the microscopic topological constraints dominating the dynamics of long-chain polymers [60]. The KG model is formulated in the natural units of the Lennard-Jones potential describing the interaction potential between beads. The energy scale ϵ together with the bead diameter, σ , and mass, m_b , define the standard Lennard-Jones system of units including the time scale $\tau = \sigma \sqrt{m_b/\epsilon}$.

The purpose of this paper is to establish KG simulations as a convenient tool for exploring emergent universal properties of *specific* polymer materials. To obtain valid coarse-grain descriptions for commodity polymer melts, we tune the strength of a bending potential introduced into the model by Faller and Müller-Plathe[61–63]. The proposed mapping relies on results of a preceding paper, where we have studied the dependence of the characteristic time and length scales in KG bead-spring polymer melts on this parameter [64]. Here we provide tables specifying a one-parameter KG force field for a wide range of experimental polymer melts, i.e. we list which bending stiffness to use for a particular polymer and how to translate KG into SI units.

The paper is structured as follows; We introduce the Kuhn scale in Sec. II, where we also express a number of chemical polymers (IIB) and KG model polymers with varying chain stiffness (IIC) in Kuhn units. We also derive mapping relations for static (IID) and dynamic (IIE) properties, and discuss transferability (IIF). In Sec. III, we use polymer theory to illustrate that two polymer samples characterized by the same two numbers are expected to display the same emergent properties beyond the Kuhn scale. We also give a concrete example in the case of the entanglement modulus for KG models of varying stiffness matches that of chemical polymers. Finally, we briefly conclude in Sec. V.

II. MATCHING AT THE KUHN SCALE

The natural units of polymer physics [3, 4, 65] are the mesoscopic Kuhn units: the Kuhn length, l_K , the Kuhn time, τ_K , and $k_B T$ as the natural energy scale in entropy dominated systems. Kuhn’s seminal insight in the 1930s was to use an N_K step random walk of segment length l_K as a coarse-grain description of its large scale conformations [66]. For the proper choice of l_K , the Kuhn model reproduces both, the end-to-end distance at full extension, $L = l_K N_K$, and the mean-square end-to-end distance, $\langle R^2 \rangle = N_K l_K^2$, of the target polymer. In particular, flexible polymers exhibit *universal* behavior [3, 4, 65] beyond the Kuhn scale defined by l_K and the corresponding time scale τ_K . In contrast, behavior on smaller scales is material specific and dependent on atomic detail. For example, the large scale flexibility has completely different microscopic origins in the wormlike chain [67] and in the rotational-isomeric-state [2] models. Similarly, there are well-documented exceptions [68] to the strong form

of time-temperature superposition principle, which postulates identical temperature dependence for all microscopic relaxation mechanisms down to the atomic scale. When it comes to linking theory, experiments, atomistic and coarse-grain simulation, then we believe that the natural approach is to match them at the Kuhn scale.[69]

A. The Kuhn scale

The Kuhn length,

$$l_K = \frac{\langle R^2 \rangle}{L}, \quad (1)$$

characterizes the crossover from local rigid rod to random walk behavior.

It is not straightforward to infer the Kuhn length from the chemical structure of a polymer in its melt state as it depends on intramolecular interactions, chemistry-specific local packing, and universal long-range correlations[2, 42]. However, a known Kuhn length can be used to characterize the large scale structure of polymer melts via two related dimensionless numbers.

The first such number is a dimensionless measure of chain length, the number of Kuhn segments per chain:

$$N_K = \frac{\langle R^2 \rangle}{l_K^2} = \frac{L^2}{\langle R^2 \rangle}, \quad (2)$$

The second number, to which we refer as the Kuhn number, is a dimensionless measure of density,

$$n_K = \rho_K l_K^3, \quad (3)$$

defined as the number of Kuhn segments within the volume of a Kuhn length cube.

To characterise the dynamics, one can define the friction coefficient, ζ_K , of a Kuhn segment undergoing Brownian motion. Interpreting ζ_K as a viscous Stokes drag, $\zeta_K \propto \eta_K l_K$, it is convenient to define an effective viscosity at the Kuhn scale as

$$\eta_K = \frac{1}{36} \frac{\zeta_K}{l_K}. \quad (4)$$

The fundamental time scale of the dynamics of intrinsically flexible polymers is set by time that it takes a single Kuhn segment to diffuse ($D_K = k_B T / \zeta_K$) its own size. Again it turns out to be practical to incorporate some numerical prefactors into the definition of the Kuhn time:

$$\tau_K = \frac{1}{3\pi^2} \frac{\zeta_K l_K^2}{k_B T} = \frac{12}{\pi^2} \frac{\eta_K l_K^3}{k_B T}. \quad (5)$$

B. Commodity polymer melts at the Kuhn scale

At a given state point (temperature), a melt of monodisperse chains (with molecular weight M_c) can be

name	T_{ref}/K	n_K	$l_K/\text{\AA}$	$M_K/[g/mol]$	M_K/M_m	$\rho_K/[nm^{-3}]$	$p/\text{\AA}$	$d_T/\text{\AA}$	d_T/p	$Ge l_K^3/[k_B T]$	N_{eK}
PI-50	298	2.50	8.80	146.60	2.15	3.66	3.52	47.7	13.6	0.068	36.76
PI-7	298	2.72	8.44	119.60	1.76	4.52	3.10	55.1	17.8	0.051	53.19
PDMS*	298	2.82	11.42	309.28	4.17	1.89	4.06	63.7	15.7	0.072	38.85
PI-20	298	2.86	8.98	136.50	2.00	3.95	3.13	54.8	17.5	0.062	46.46
PI-34	298	3.02	9.58	156.90	2.30	3.44	2.94	56.5	19.2	0.075	40.40
cis-PBd	298	3.40	8.28	90.50	1.67	5.99	2.43	42.2	17.3	0.105	32.42
PIB(413)	413	3.47	12.20	267.90	4.77	1.91	3.51	65.8	18.7	0.096	36.27
cis-PI	298	3.47	9.34	128.60	1.89	4.26	2.69	46.0	17.1	0.115	30.19
a-PP(463)	463	3.53	11.20	183.40	4.36	2.51	3.20	61.7	19.3	0.092	38.24
i-PP	463	3.64	11.40	187.80	4.46	2.46	3.12	61.7	19.8	0.100	36.53
a-PP(413)	413	3.65	11.20	183.40	4.36	2.60	3.10	56.0	18.1	0.116	31.51
a-PP(348)	348	3.81	11.20	183.40	4.36	2.71	2.97	51.9	17.5	0.140	27.13
a-PP	298	3.92	11.20	183.40	4.36	2.79	2.87	48.8	17.0	0.164	23.94
PIB	298	3.94	12.50	274.20	4.89	2.02	3.17	55.2	17.4	0.161	24.40
a-PMMA	413	4.07	15.30	598.00	5.97	1.14	3.77	62.5	16.6	0.195	20.90
i-PS*	413	4.19	17.11	697.12	6.69	0.84	4.08	76.7	18.8	0.167	25.12
a-PMA	298	4.29	14.70	494.60	5.75	1.35	3.43	61.9	18.1	0.193	22.24
PI-75	298	4.53	15.00	399.30	5.86	1.34	3.31	51.8	15.6	0.304	14.93
PBd-20	298	4.54	10.10	122.40	2.26	4.41	2.21	37.3	16.9	0.268	16.94
a-PS*	413	4.54	17.80	725.34	6.96	0.80	3.92	76.3	19.4	0.198	22.94
PBd-98	300	4.83	13.70	284.80	5.27	1.88	2.82	45.4	16.1	0.354	13.66
PEO*	353	4.99	9.71	117.12	2.66	5.45	1.95	33.4	17.1	0.338	14.76
POM*	473	5.06	9.65	122.11	4.07	5.62	1.91	40.1	21.0	0.234	21.60
a-PHMA	373	5.19	24.40	1622.00	9.53	0.36	4.73	98.4	20.8	0.254	20.44
a-PVA*	333	5.26	16.50	555.70	6.45	1.17	3.14	57.9	18.4	0.342	15.37
SBR	298	5.33	11.90	173.60	2.61	3.16	2.22	43.6	19.6	0.319	16.69
P6N*	543	5.53	10.93	140.05	1.24	4.24	1.98	41.1	20.8	0.314	17.64
a-P α MS*	473	5.66	20.43	944.61	7.99	0.66	3.61	67.2	18.6	0.418	13.53
a-PEA	298	5.70	18.10	710.10	7.09	0.96	3.17	53.7	16.9	0.519	10.99
PET*	548	7.50	14.91	263.15	1.37	2.26	1.99	31.3	15.8	1.359	5.52
s-PP	463	7.99	16.90	278.70	6.62	1.66	2.10	42.4	20.2	1.019	7.84
PE(413)	413	8.09	13.70	150.40	5.36	3.14	1.69	32.2	19.0	1.172	6.90
a-POA	298	8.34	31.90	2295.00	12.45	0.26	3.83	73.3	19.1	1.262	6.61
PC*	473	10.93	18.43	393.25	1.55	1.75	1.69	33.9	20.1	2.589	4.22
PE	298	11.10	15.40	168.30	6.00	3.04	1.39	26.0	18.6	3.107	3.57
PTFE*	653	12.30	23.40	915.41	9.15	0.96	1.90	47.2	24.8	2.415	5.09

TABLE I: Kuhn descriptions of polymers in terms of Kuhn number n_K , Kuhn length l_K , mass of a Kuhn segment M_K , Kuhn density ρ_K , packing length p , tube diameter d_T , p/d_T , the reduced entanglement modulus $Ge l_K^3/[k_B T_{ref}]$, and finally Kuhn segments between entanglements N_{eK} . * denotes polymers where we have derived the Kuhn scale descriptions as in Ref. [70]. When necessary we have added the reference temperature to the polymer name when the same polymer species has been characterized at multiple temperatures.

characterized by just a few experimental observables: the mass density ρ_{bulk} , the average chain end-to-end distance per unit mass $\langle R^2 \rangle / M_c$, and the maximal chain extension, L . Values for these observables a large number of typical polymers are collected in Ref. [70]. We present a selected subset of polymers expressed in Kuhn units in Tab. I. The Kuhn lengths are in the 1 – 2 nanometer range, with a Kuhn segment mass $M_K = M_c / N_K \sim$

100 – 2000 g/mol. The number of monomers in a Kuhn segment varies in the range of 1 – 13, and the Kuhn density varies in the range of 0.5 – 5 nm^{-3} . The packing length is derived from the bulk density and end-to-end distance, while the entanglement modulus and bulk density provides an estimate for the tube diameter. While these two observables varies from polymer to polymer, their ratio is roughly constant for all flexible

polymers.[71, 72]

The key property of a chemical polymer species are their Kuhn number, which varies in the range 2 – 12 for flexible polymers. We observe no systematic correlations between the Kuhn properties of a polymer and the Kuhn number, because they depend on chemistry specific details. However, emergent properties such as the entanglement modulus and hence entanglement length displays a strong and systematic correlation with the Kuhn density. For comparison, $n_K \gg 10$ in gels of tightly entangled filamentous proteins such as f-actin.[73]

C. Kremer-Grest model polymer melts at the Kuhn scale

The Kremer-Grest model[59, 60] is a defacto standard model in Molecular Dynamics investigations of generic polymer properties. The KG model is a bead-spring model, where the mutual interactions between all beads are given by the Weeks-Chandler-Anderson (WCA) potential (the truncated and shifted repulsive part of the 12-6 Lennard-Jones potential),

$$U_{WCA}(r) = 4\epsilon \left[\left(\frac{\sigma}{r}\right)^{-12} - \left(\frac{\sigma}{r}\right)^{-6} + \frac{1}{4} \right] \quad \text{for } r < 2^{1/6}\sigma, \quad (6)$$

where ϵ defines the energy scale and σ the bead diameter. The standard choice for the temperature is $k_B T = \epsilon$. Bonded beads interact through the finite-extensible-non-linear spring (FENE) potential given by

$$U_{FENE}(r) = -\frac{kR^2}{2} \ln \left[1 - \left(\frac{r}{R}\right)^2 \right]. \quad (7)$$

Choosing a spring constant $k = 30\epsilon\sigma^{-2}$ and a bond length, $R = 1.5\sigma$, where the FENE potential diverges, the bond length is $l_b = 0.965\sigma$. The standard choice for the bead density is $\rho_b = 0.85\sigma^{-3}$ Faller and Müller-Plathe [61–63] augmented the standard KG model with a bending potential,

$$U_{bend}(\Theta) = \kappa(1 - \cos \Theta), \quad (8)$$

where Θ denotes the angle between subsequent bonds.

To prepare the present study, we have recently investigated the dependence of the characteristic time and length scales in KG bead-spring polymer melts on the scale of the bending energy, $x \equiv \beta\kappa = \kappa/k_B T$ [64]. In particular, we found for the Kuhn length:

$$\begin{aligned} l_K &= l_K^{(0)} + \Delta l_K \quad (9) \\ l_K^{(0)}/\sigma &= \frac{l_b}{\sigma} \begin{cases} \frac{2x + e^{-2x} - 1}{1 - e^{-2x}(2x+1)} & \text{if } x \neq 0 \\ 1 & \text{if } x = 0 \end{cases} \\ \Delta l_K/\sigma &= 0.769888 + 0.776514 \times \\ &\quad \tanh(0.147244 - 0.405299x - 0.0298337x^2) \end{aligned}$$

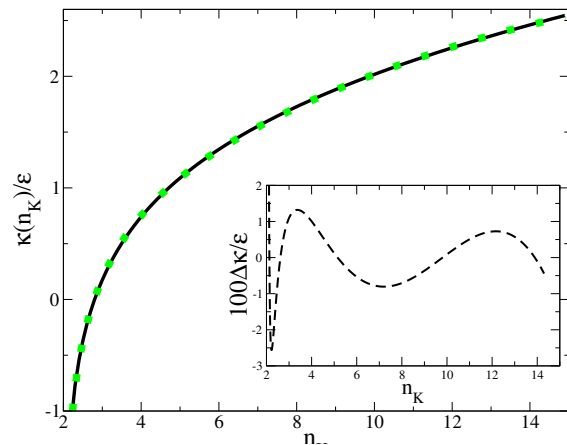


FIG. 1: KG chain stiffness vs. Kuhn number using eq. (10) (solid black line) and our approximate inversion eq. (15) (green symbols). The inset shows the error of our numerical inversion.

From this relation, we can directly infer the dimensionless Kuhn number, Eq. (3), characterising KG melts:

$$n_K(\beta\kappa) = \rho_b \frac{l_b}{l_K} l_K^3. \quad (10)$$

Finally, the number of Kuhn segments between entanglements, the Kuhn friction and Kuhn time of the KG model are given by

$$N_{eK} = 39.130 - 30.237x + 4.2834x^2 + 3.2065x^3 - 1.2879x^4 + 0.1372x^5 \quad (11)$$

$$\zeta_K/(m_b/\tau) = 36.021 + 10.149x + 5.6341x^2 \quad (12)$$

$$\tau_K/\tau = 4.2076 + 2.8451x + 1.6485x^2 + 0.6464x^3 + 0.6524x^4 \quad (13)$$

The parameterization of the Kuhn length we believe to be valid for arbitrary values for stiffness κ , while the expressions above are valid for the chain stiffness in the interval $-1 < \beta\kappa < 2.5$.

D. A one parameter Kremer-Grest “force field” for commodity polymer melts

As a first step in defining a KG force field for a polymeric material we fix the energy scale to the thermal excitation energy [74],

$$\epsilon = k_B T^{exp}. \quad (14)$$

The key step is the choice of the bending stiffness: we match the dimensionless Kuhn numbers n_K characterising the experimental system and the model polymer melt. A priori, this requires the numerical inversion of the combination of Eqs. (9) and (10). As shown in Fig. 1, the

approximate relation

$$\frac{\kappa(n_K)}{k_B T} = 0.822264 \log(n_K - 2.) - 0.000290834 n_K^3 + 0.00871154 n_K^2 - 0.0552417 n_K + 0.280663 \quad (15)$$

provides an excellent approximation over the experimentally relevant range, $2 \leq n_K \leq 15$. Hence in the following we regard the KG Kuhn parameters as being functions of the Kuhn number rather than the bending stiffness of the KG model. Note that the standard KG model with $\beta\kappa = 0$ essentially corresponds to the intrinsically most flexible polymers such as PDMS or PI with 7 – 50% 3,4 content.

Rewriting Eq. (10), we can obtain the number of beads per Kuhn length

$$c_b(n_K) \equiv \frac{l_K}{l_b} = \sqrt{\frac{n_K}{\rho_b l_b^3}} \quad (16)$$

and hence the number of beads required to represent a chain of a given length

$$N_b = c_b(n_K) N_K . \quad (17)$$

What remains is to fix the mapping relations for the simulation units of length, mass, and time. Equating the model and experimental Kuhn lengths and accounting for the small difference, $l_b = 0.965\sigma$, between the bond length and the bead diameter in the KG model, we obtain

$$\sigma = \frac{l_K^{exp}}{0.965 \times c_b(n_K)} \quad (18)$$

The bead mass is obtained along the same lines by equating the experimental mass of a Kuhn segment to the mass of a Kuhn segment in the model:

$$m_b = \frac{M_K^{exp}}{c_b(n_K)} . \quad (19)$$

Using the relations presented above, we have generated Kremer-Grest model parameters and mappings for most of the polymer species shown in Tab. I, the mapping relations are shown in Tab. II. From the mapping relations, we note that the only free parameter, the stiffness parameter varies from $\kappa = -0.38\epsilon$ up to $\kappa = 2.29\epsilon$, which falls into the range where our empirical relations for Kuhn length, entanglement length, and Kuhn friction are valid.

From the mappings we note that the number of beads per monomer produced by the mapping is about 1.2 to 13. The length scale of the beads is between 4 and 10Å, the energy scale is by construction always kT . Despite fairly small variations in the length and energy scales, the unit of stress $\epsilon\sigma^{-3}$ is quite sensitive to the specific polymer species and varies between 17 and 111MPa, which is quite important when using KG models to predict the viscoelastic properties of real polymers.

E. Time mapping

Above we have provided a mapping from real polymers to KG model polymers that we expect will reproduce the same static conformational properties and hence observables. What about dynamical properties? This requires a mapping relation between the simulation time unit τ and an experimental time unit.

We have previously obtained the Kuhn time of the KG model as function of stiffness and used it to predict all the time scales of polymer dynamics, and shown good agreement agreement up to and beyond the Rouse time. [64] Using eq. (13), we can predict the Kuhn time $\tau_K(n_K)$ in units of τ as function of the Kuhn number. Furthermore using eq. (11), the entanglement time is predicted as $\tau_e(n_K) = N_{eK}(n_K)^2 \tau_K(n_K)$. The Rouse time is $\tau_R(n_K) = N_K^2 \tau_K(n_K)$. Finally the terminal relaxation time is $\tau_{max}(n_K) = 3N_K^3 \tau_K(n_K) / N_{eK}(n_K)$. Note that for finite chain lengths the terminal relaxation time will be significantly affected by contour-length fluctuations and constrain release.[3, 80, 83]

Different experiments can be used to probe the polymer dynamics. The Kuhn time τ_K can be obtained from neutron spin echo experiments whereas the entanglement time $\tau_e(\kappa) = \tau_K(\kappa) N_{eK}^2(\kappa)$ can be measured by transverse relaxation NMR measurements. Oscillatory rheological experiments can when applying the time-temperature superposition assumption cover most of this dynamical range in frequency space. For reviews of these experimental techniques see e.g. Refs. [84–88].

To accurately estimate a characteristic times scale often a model needs to be fitted to experimental data. Secondly, the experimental time scale should be determined at the same state point as that used for the conformational properties, alternatively one can attempt to use time-temperature superposition to shift an experimental time scale to the same temperature as the conformational input. Fitting models can introduce systematic errors due to the approximate nature of the models. An alternative route to obtain a time mapping is e.g. from viscosity data of unentangled melts of varying chain length where we can estimate the time mapping using eqs. (21, 5).

In Tab. III we have collected some estimates for entanglement times from various experiments to obtain time mapping relations. For some of the polymers we have assumed the time-temperature superposition (TTS)[79] to shift the entanglement times to the reference temperature used to estimate the chain stiffness. We observe that 1τ varies in a huge range from 5ps up to 50μs for the present polymers. This is in reasonable agreement with $1\tau \sim 2ps - 31ns$ range estimated by Kremer and Grest[60]. For the polymers where we have mapping data at several temperatures, we can clearly see that as the temperature is reduced the real time corresponding to 1τ grows significantly towards the glass transition temperature. For a-PS (413K) and a-PP (298K), the polymers are just about 40 degrees above the glass transition tem-

name	n_K	$\beta\kappa$	c_b	l_K/σ	M_m/m_b	$m_b/[g/mol]$	$\epsilon/10^{-21}J$	σ/nm	$\epsilon\sigma^{-3}/MPa$
PI-50	2.50	-0.378	1.81	1.74	2.15	81.13	4.11	0.50	32.0
PI-7	2.72	-0.086	1.89	1.82	1.76	63.37	4.11	0.46	41.3
PDMS*	2.82	0.013	1.92	1.85	4.17	161.05	4.11	0.62	17.6
PI-20	2.86	0.056	1.94	1.87	2.00	70.50	4.11	0.48	37.1
PI-34	3.02	0.191	1.99	1.92	2.30	78.86	4.11	0.50	33.1
cis-PBd	3.40	0.445	2.11	2.04	1.67	42.87	4.11	0.41	61.3
PIB(413)	3.47	0.483	2.13	2.06	4.77	125.69	5.70	0.59	27.3
cis-PI	3.47	0.484	2.13	2.06	1.89	60.32	4.11	0.45	44.0
a-PP(463)	3.53	0.518	2.15	2.07	4.36	85.25	6.39	0.54	40.7
i-PP	3.64	0.575	2.18	2.11	4.46	85.96	6.39	0.54	40.4
a-PP(413)	3.65	0.580	2.19	2.11	4.36	83.84	5.70	0.53	38.2
a-PP(348)	3.81	0.656	2.23	2.16	4.36	82.08	4.80	0.52	34.3
a-PP	3.92	0.708	2.27	2.19	4.36	80.84	4.11	0.51	30.7
PIB	3.94	0.714	2.27	2.19	4.89	120.66	4.11	0.57	22.2
a-PMMA	4.07	0.770	2.31	2.23	5.97	258.82	5.70	0.69	17.6
i-PS*	4.19	0.819	2.35	2.26	6.69	297.22	5.70	0.76	13.2
a-PMA	4.29	0.856	2.37	2.29	5.75	208.42	4.11	0.64	15.6
PI-75	4.53	0.941	2.44	2.35	5.86	163.78	4.11	0.64	15.9
PBd-20	4.54	0.944	2.44	2.35	2.26	50.16	4.11	0.43	52.2
a-PS*	4.54	0.944	2.44	2.35	6.96	297.19	5.70	0.76	13.2
PBd-98	4.83	1.039	2.52	2.43	5.27	113.08	4.14	0.56	23.1
PEO*	4.99	1.086	2.56	2.47	2.66	45.77	4.87	0.39	80.2
POM*	5.06	1.105	2.58	2.48	4.07	47.40	6.53	0.39	111.5
a-PHMA	5.19	1.143	2.61	2.52	9.53	621.59	5.15	0.97	5.7
a-PVA*	5.26	1.162	2.63	2.53	6.45	211.52	4.60	0.65	16.7
SBR	5.33	1.182	2.65	2.55	2.61	65.62	4.11	0.47	40.6
P6N*	5.53	1.234	2.69	2.60	1.24	51.98	7.50	0.42	100.9
a-P α MS*	5.66	1.265	2.72	2.63	7.99	346.66	6.53	0.78	13.9
a-PEA	5.70	1.276	2.74	2.64	7.09	259.56	4.11	0.69	12.8
PET*	7.50	1.646	3.14	3.03	1.37	83.82	7.57	0.49	63.4
s-PP	7.99	1.728	3.24	3.12	6.62	86.03	6.39	0.54	40.5
PE(413)	8.09	1.744	3.26	3.14	5.36	46.15	5.70	0.44	69.0
a-POA	8.34	1.785	3.31	3.19	12.45	693.22	4.11	1.00	4.1
PC*	10.93	2.136	3.79	3.65	1.55	103.76	6.53	0.50	51.0
PE	11.10	2.156	3.82	3.68	6.00	44.07	4.11	0.42	56.4
PTFE*	12.30	2.291	4.02	3.87	9.15	227.70	9.02	0.60	41.1

TABLE II: Kremer-Grest model parameters for the polymers shown in Tab. I in terms of the Kuhn number, bending stiffness $\beta\kappa$, number of beads per Kuhn segment c_b , Kuhn length expressed in KG units, number of beads per monomer M_m/m_b , and finally the conversion relations from KG units for energy ϵ , length σ , and stress $\epsilon\sigma^{-3}$ to SI units.

perature. Interestingly PIB (298K) also has a very large time mapping despite being 100 degrees above the glass transition temperature. Perhaps this can be explained by intramolecular rotational barriers to relaxation dynamics specific for PIB, which has also been studied experimentally for this polymer.[89].

F. Transferability

What happens if we change to a different state point (temperature)? Typically the static melt properties are relatively insensitive to changes of temperature: the relative density expansion coefficient is $d \ln \rho_{bulk}/dT \approx -6 \times 10^{-4} K^{-1}$, while typical thermal chain expansion coefficients $|d \ln \langle R^2 \rangle(T)/dT| < 10^{-3} K^{-1}$. [70] Since $n_K(T) \sim \rho_{bulk} \langle R^2 \rangle^2$, we obtain $|d \ln n_K(T)/dT| < 3 \times 10^{-3} K^{-1}$. This indicates that we can expect the present approach

name	T_{ref}/K	τ_K/τ	τ_e/τ	τ_c^{exp}/s	τ/ps
PI-7	298	3.9	6872	$1 - 3 \times 10^{-5}$	2000 – 4000
PDMS	298	4.2	6290	$7 - 10 \times 10^{-8}$	10 – 20
cis-PDb	298	5.8	4174	$4 - 8 \times 10^{-8}$	10 – 20
cis-PI	298	6.0	4014	$3 - 6 \times 10^{-6}$	800 – 1700
cis-PI (2)	298	6.0	4014	13.2×10^{-6}	3000
a-PP	463	6.2	3879	$2.2 - 2.4 \times 10^{-8}$	6 – 7
i-PP	463	6.6	3661	$3.5 - 9.9 \times 10^{-8}$	10 – 27
a-PP	413	6.6	3642	$5.2 - 5.6 \times 10^{-8}$	14 – 15
a-PP	348	7.1	3367	$5.3 - 5.7 \times 10^{-7}$	145 – 157
a-PP	298	7.4	3189	$1.1 - 1.2 \times 10^{-4}$	$3.1 - 3.3 \times 10^4$
PIB	298	7.5	3169	1.7×10^{-3}	5.3×10^5
a-PS	413	9.5	2479	0.13 – 0.14	$5.1 - 5.8 \times 10^7$
PEO	348	11.0	2123	$1.5 - 2.3 \times 10^{-8}$	7 – 10
PE	413	23.6	1071	$3 - 15 \times 10^{-9}$	3 – 14
PE	298	38.5	797	$5 - 26 \times 10^{-8}$	70 – 320

TABLE III: Polymer dynamics: Experimental entanglement times for some of the polymers in Tab. I. References for data: PI-7 [75], PDMS, cis-PDb, cis-PI [76] using $\kappa = 3\pi^2$ using TTS parameters from the reference, cis-PI (2)[77], a-PP [78] shifted with TTS parameters from [79], i-PP, PIB [78], a-PS [80] TTS parameters from [79], PEO [81], and PE [82] TTS shifted with an Arrhenius relation also from the reference.

to be quite transferable. Assuming the temperature dependence of the end-to-end distance and bulk density is known, then we can use the expressions stated above to predict the bending stiffness of the resulting KG model as well as new mapping relations for converting simulation units to SI units.

While static observables does not change significantly with temperature, the time mapping is strongly temperature dependent. Note simulations are always performed at a reduced temperature $T = 1$, because we choose $\epsilon = k_B T_{ref}$ as our unit of energy in simulations. Assuming $\tau_c^{exp}(T_{ref})$ to be an experimental time scale measured at temperature T_{ref} , from time-temperature superposition we expect

$$\tau_c^{exp}(T) = \frac{\tau_c^{exp}(T_{ref})}{a_T} = \tau_c^{KG}$$

with $\log a_T = \frac{-C_1(T-T_{ref})}{C_2+T-T_{ref}}$ [90]. Hence we can expect an exponential acceleration of real time vs. one unit of simulation time as the experimental temperature is decreased relative to the reference temperature.

III. PREDICTING EMERGENT UNIVERSAL BEHAVIOR BEYOND THE KUHN SCALE

The separation of characteristic time and length scales in polymeric systems can be substantial. To take the example of natural rubber (*cis*-PI) with a Kuhn length below the nanometer scale (see Table I), chains composed of $N_K = 10^4$ Kuhn segments reach contour lengths in the

μm range and coil diameter of the order of 100 nm. Having completed the matching of experimental systems and KG model polymer melts at the Kuhn scale, an obvious question arises: do we have reasons to believe, that this is “enough” to describe the emergent behavior on much larger scales?

In the following, we provide a brief outline of polymer theory [3, 4, 65, 91] to argue that this is indeed the case. The point of the exercise is to illustrate, that two monodisperse polymer melts are expected to show the same universal large scale behavior, provided (i) they are characterized by the same number of Kuhn segments per chain, N_K , and the same dimensionless Kuhn density, n_K , and (ii) properties are measured in the “natural” Kuhn units. Our KG models can be expected to have predictive power for emergent polymer properties, if we may take it for granted that this universality extends to a computational model that exhibits the key features of polymer melts: chain connectivity, local liquid-like monomer packing, and the impossibility of chain backbones to dynamically cross through each other.

We begin our short *tour d’horizon* with the Rouse model [3, 92], which describes the dynamics of short unentangled polymers. Rouse considered the Langevin dynamics of a “Gaussian” chain composed of beads, which experience local friction and which are connected by harmonic springs representing the entropic elasticity of polymer sections beyond the Kuhn scale. In this model, the maximal internal relaxation time of a chain is given by the Rouse time

$$\tau_R = N_K^2 \tau_K, \quad (20)$$

while the macroscopic melt viscosity can be written as

$$\eta = n_K N_K \eta_K . \quad (21)$$

For the example of natural rubber, $\tau_R \sim 10^8 \tau_K$, is a *macroscopic* time scale, while this initial estimate of the melt viscosity yields $\eta \sim 4 \times 10^4 \eta_K$.

The key for understanding the properties of polymer melts is the realisation, that chains strongly interpenetrate. The Flory number, $n_F = \rho_c \langle R^2 \rangle^{3/2}$, is defined as the number of chains populating, on average, the volume spanned by one chain. That the Flory number is large, explains why chains behave nearly ideally in a melt [2] and why polymer systems can often be well described by mean-field theories [93, 94]. For our present purposes, it is important to note that n_F and hence the degree of this interpenetration can again be simply expressed as a sole function of the two dimensionless numbers characterising a melt on the Kuhn scale:

$$n_F = n_K N_K^{1/2} \quad (22)$$

or $n_F \sim 400$ for natural rubber.

Chains undergoing Brownian motion can slide past each other, however, their backbones cannot cross[3]. As a consequence, the motion of long chains is subject to long-lived topological constraints[95]. Modern theories of polymer dynamics [3] are based on the idea that molecular entanglements confine individual filaments to a one-dimensional, diffusive motion (reptation [96]) in tube-like regions in space [97]. The constraints become relevant at scales beyond the entanglement (contour) length[98, 99], L_e , or the equivalent the number of Kuhn units between entanglements, $N_{eK} = L_e/l_K$. According to the packing argument for loosely entangled polymers [71–73], there are

$$N_{eK} = \left(\frac{\alpha}{n_K} \right)^2 \quad (23)$$

Kuhn segments per entanglement length. The (spatial) tube diameter is given by

$$\frac{d_T}{l_K} = \sqrt{\frac{\langle R^2(N_{eK}) \rangle}{l_K^2}} = \sqrt{N_{eK}} = \frac{\alpha}{n_K} \quad (24)$$

while

$$\tau_e = \tau_K N_{eK}^2 = \tau_K \left(\frac{\alpha}{n_K} \right)^4 \quad (25)$$

defines the corresponding entanglement time, beyond which the Rouse model fails to describe dynamic correlations. Again, the point to note is, that when defined in Kuhn units, the entanglement scale only depends on the Kuhn number, n_K , since the number of entanglement strands per entanglement volume,

$$\alpha = \frac{\rho_K}{N_{eK}} d_T^3 = 18 \pm 2 , \quad (26)$$

appears to be a universal constant for all flexible polymers [71, 72, 100, 101].

In the limit of long chains the reduced maximal relaxation time is [96] is $\tau_{max} = 3Z^3 \tau_e$, where $Z = N_K/N_{eK}$ denotes the number of entanglements per chain. Using Eq. (23), we see that

$$Z = \frac{n_K^2 N_K}{\alpha^2} \quad (27)$$

only depends on dimensionless constants, which are reproduced in KG melts parameterized at the Kuhn scale. As a consequence, the correct of number of entanglements emerges from the microscopic topological constraints in the KG melts, suggesting that they also exhibit the same asymptotic maximal relaxation time as the experimental target systems:

$$\tau_{max} = 3Z^3 \tau_e = 3 \frac{n_K^2 N_K^3}{\alpha^2} \tau_K . \quad (28)$$

In slowing down the chain equilibration after a deformation, entanglements dominate the viscoelastic behavior of high molecular weight polymeric liquids. For $\tau_e < t < \tau_{max}$ the shear relaxation modulus, $G(t)$ exhibits a rubber-elastic plateau, $G_N = \frac{4}{5} G_e$, of the order of the entanglement modulus,

$$\frac{G_e l_K^3}{k_B T} = \frac{\rho_K l_K^3}{N_{eK}} = \frac{n_K^3}{\alpha^2} . \quad (29)$$

Figure 2 shows the reduced entanglement moduli as a function of Kuhn number. The experimental data are in very good agreement with our prediction eq. (29) for flexible chains. For large Kuhn numbers, we expect a cross-over to tightly entangled behaviour.[73] We have made a semi-empirical expression[64] that appears to be in slightly better agreement with the experimental data.

Figure 3 shows a comparison between experimental plateau moduli and entanglement moduli of KG melts extracted from Primitive Path Analysis [64, 83]. Most of the experimental values are within the 30% error interval around the KG models. The scatter observed between the experimental plateau moduli and the predicted plateau modulus line must be attributed either to chemical details causing some small degree of non-universal behaviour[102], such as a non-negligible crystalline fraction, or to experimental uncertainties in accurately estimating the plateau modulus which can be quite difficult.[103] We also observe an excellent agreement between our semi-empirical prediction and the KG models. The KG models are clearly able to predict the entanglement modulus of the chemical polymer species with good accuracy.

The time integral of the shear relaxation modulus is the melt viscosity. The asymptotically expected result [3] can be written as

$$\eta = \frac{\pi^2}{15} G_e \tau_{max} = \frac{2}{5} \frac{n_K^5 N_K^3}{\alpha^3} \eta_K . \quad (30)$$

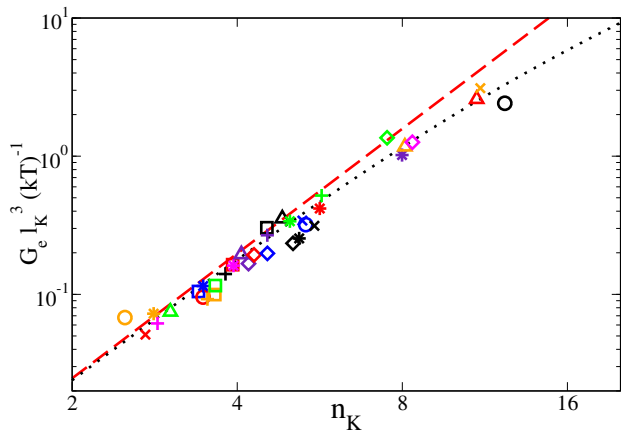


FIG. 2: Reduced entanglement moduli for the polymers in Tab. I compared to the theoretical expectation for flexible polymers eq. (29) (red dashed line) to our the semi-empirical prediction of eq. (42) in Ref. [64]) (black dotted line) The symbols denote in order of increasing Kuhn number: PI-50 (orange \circ), PI-7 (red \times), PDMS (orange $*$), PI-20 (magenta $+$), PI-34 (green Δ), cis-PBd (blue \square), PIB(413) (red \circ), cis-PI (blue $*$), a-PP(463) (orange $+$), i-PP (orange \square), a-PP(413) (green \square), a-PP(348) (black $+$), a-PP (red \square), PIB (magenta $*$), a-PMMA (indigo Δ), i-PS (indigo \diamond), a-PMA (red \diamond), PI-75 (black \square), PBd-20 (indigo $+$), a-PS (blue \diamond), PBd-98 (black Δ), PEO (green $*$), POM (black \diamond), a-PHMA (black $*$), a-PVA (blue \times), SBR (blue \circ), P6N (black \times), h a-PAMS (red $*$), a-PEA (green $+$), PET (green \diamond), s-PP (indigo $*$), PE(413) (orange Δ), a-POA (magenta \diamond), PC (red Δ), PE (orange \times), and PTFE (black \circ).

suggesting that this property should also be quantitatively reproduced by our KG models. We also expect simulations to completely account for relaxation processes such as contour length fluctuations and constraint release. [83] These effects renormalize the maximal relaxation time and shear relaxation modulus, but in a way that only depends on Z [3, 86] and hence also has a universal dependence on the Kuhn number and the number of Kuhn units per polymer.

To model entanglement effects in the linear regime, one does not necessarily need to descend to the Kuhn scale. However, strong deformations drive chains to their maximal extension, which for long chains is given by $\sqrt{N_e K}$ and is thus properly accounted for in our KG models. Furthermore is tempting to speculate, that the friction reduction in fast elongational flows attributed to the alignment of the Kuhn segments to the stretching direction[104] might naturally emerge in KG melts, extending their applicability from the linear regime deep into the nonlinear regime.[105]

IV. DISCUSSION

Kremer and Grest[60] were the first to discuss how to compare the KG model to experiment. They did not

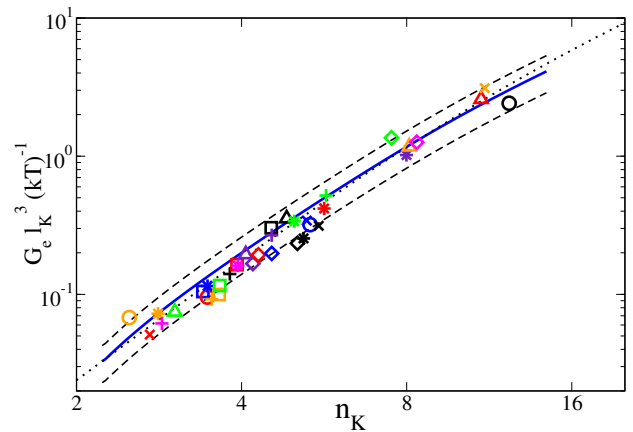


FIG. 3: Reduced entanglement moduli for the experimental data in Fig. 2 compared to the range of KG models for $-1 \leq \beta\kappa \leq 2.5$ (blue solid line), with indications of $\pm 30\%$ error (dashed black lines). Also shown are our the semi-empirical prediction of eq. (42) in Ref. [64]) (black dotted line)

vary the stiffness, but instead matched the standard KG model ($\beta\kappa = 0$ in the present notation) with several polymers. They choose to match at the entanglement scale by identifying KG melts and experimental systems with the same number of entanglements (using the estimate $N_e = 35$ (beads between entanglements) estimated from the transition from the $t^{1/2}$ to $t^{1/4}$ behaviour of mean-square displacements, where eqs. (9, 11) give $N_e = 75$). The mapping for σ was obtained by matching the KG tube diameter to experimental tube diameters estimated from the chain statistics and plateau moduli. Finally by matching diffusion coefficients for chains in the Rouse regime, they were able to derive a time mapping. Their mapping relations for length scales and number of beads per monomer are of the order of ours.

Kröger [74] pointed out the importance of comparing dimensionless numbers when mapping, and derived mapping relations for the standard KG model by matching matching entanglement and critical molecular weight of the KG model to that of the polymer, hence he also matches simulation and experiment at the entanglement scale. Where his approach deviates from the present and that of Kremer and Grest is that he suggests to match times using the definition $\tau = \sigma \sqrt{m_b/\epsilon}$ by inserting known mapping relations for the units on the right hand side. This matches the simulation time scale to the characteristic time it takes for a bead to moves its own size by ballistic motion with the thermal velocity, which has no direct relevance for time scales of polymer physics.

Sukumaran et al.[36] compared the dimensionless ratio of Kuhn length to packing length p for the KG model to various polymers, and identified the KG model with cis-polyisoprene, and obtained mapping relations for statistic structure. We note that $l_K/p \equiv n_K$, hence their criterion for matching polymers is identical to ours.

Recently Takahashi et al.[106] developed mapping re-

lations between atomistic simulations and coarse-grained of polyethylene and polystyrene with the standard KG model, and showed that the KG model accurately could reproduce static and dynamic properties after applying a mapping relation. Their mapping relation was also derived by matching properties at the entanglement scale.

The major difference from the present approach to those presented above is that we choose the KG model that matches the Kuhn number of the target polymer species. Hence when simulating a model system with the same number of Kuhn units per chain as a experimental system, theory suggests that all static and dynamic properties related to entanglements will emerge naturally in the simulation. Hence we can fix the mapping relations between simulation units and SI units at the Kuhn scale.

Finally, Zhang et al.[107] applied the idea of universality similar to ours as a means for rapidly generating equilibrated model polymer melts. By fixing the invariant degree of polymerization ($\tilde{N} = n_K^2 N_K / c_\infty^2$ in our notation), they defined a hierarchy blob-chain polymer models at different scales with the same large-scale physical properties. Fine graining these to a Kremer-Grest model resulted in well equilibrated polymer models with varying chain stiffness and density of beads.

V. CONCLUSION

We have shown how to model homopolymer melts of specific chemical polymer species with an extension of the Kremer-Grest polymer model introduced by Fallner and Müller-Plathe.[61]. The force field has a single adjustable parameter, the chain stiffness. By matching the number of Kuhn segments and the reduced Kuhn density (also denoted Kuhn number in the present paper) of the KG polymer model to the specific polymer, we can build KG model melts of any flexible chemical polymer species. The resulting coarse-graining level is about one bead per chemical monomer or two to three beads per Kuhn segment.

We have, furthermore, produced polymer specific mapping relations for converting simulation units to SI units, such that we can use simulations of KG model materials to predict experimental results of real polymers. In the present paper, we have compared experimental plateau moduli to those predicted by simulations, and observed excellent agreement with almost all experimental values being within 30% of the simulation prediction.

Computationally the KG models are very cheap compared to atomistic detailed simulations. Based on our time mappings based on experimental estimates of entanglement times, we estimate $1\tau > 5ps$. This suggests that KG models use time steps at least a factor of 50 larger than in atomistic simulations. Furthermore, KG models require just 2 – 4 beads per Kuhn segment to model a polymer. For systems close to the glass transition, the speedup in modelling the large scale behaviour along the present lines would be exponentially larger. Compared to an atomistic model, this obviously comes at the price of losing the ability to *predict* any of the glassy behaviour.

The present approach also enables the generation of well equilibrated atomistic material models. Several fast equilibration procedures have recently been published for KG models.[107–109] These allow very well equilibrated highly entangled model materials to be generated relatively cheaply. Fine-graining a chemically-specific KG model material to a atomistic force field for the target polymer would allow atomistic detailed insights in model materials that are known to match the large-scale structural properties of the target polymer.

We have focused on the KG model with bending rigidity, because it has been used in a vast number of publications as a basis for studying generic polymer and materials physics, see e.g. [7, 8, 13] for reviews. Obviously, one could apply the same logic to bead-spring models with variable density, to models based on chains of rods rather than beads[110] or to lattice models[111] as long as these capture the relevant physics of polymers. An interesting challenge would be to parameterize a corresponding force-field for co-polymer systems or solutions. While this should, in principle, be possible at least for static properties, modelling the dynamics might no longer be as simple as adjusting a single time scale. Similarly, predicting the behavior of glassy or semi-crystalline polymers is beyond the scope of force-fields parameterized to reproduce universal properties.

Acknowledgments

Acknowledgement: The simulations in this paper were carried out using the LAMMPS molecular dynamics software.[112] Computation/simulation for the work described in this paper was supported by the DeiC National HPC Center, University of Southern Denmark, Denmark.

-
- [1] P. J. Flory, *Principles of polymer chemistry* (Cornell University Press, Ithaca N.Y, 1953).
 - [2] P. Flory and M. Volkenstein, *Statistical mechanics of chain molecules* (1969).
 - [3] M. Doi and S. F. Edwards, *The Theory of Polymer Dynamics* (Clarendon, Oxford, 1986).
 - [4] P. G. de Gennes, *Scaling Concepts in Polymer Physics* (Cornell University Press, Ithaca NY, 1979).
 - [5] C. Peter and K. Kremer, *Faraday Discuss.* **144**, 9 (2010).
 - [6] K. Binder, *Monte Carlo and Molecular Dynamics simulations in polymer science* (Oxford University Press: New York, 1995).
 - [7] K. Kremer, in *Soft and fragile matter: Non equilibrium*

- dynamics, metastability and flow*, edited by M. E. Cates and M. R. Evans (J. W. Arrowsmith Ltd., Bristol, U.K., 2000), p. 145.
- [8] K. Kremer, *Macromol. Chem. Phys.* **204**, 257 (2003).
 - [9] F. Müller-Plathe, *Soft Mater.* **1**, 1 (2002).
 - [10] F. Müller-Plathe, *Chem. Phys. Chem.* **3**, 754 (2002).
 - [11] Q. Sun and R. Faller, *Comput. Chem. Eng.* **29**, 2380 (2005).
 - [12] C. Tzoumanekas and D. N. Theodorou, *Curr. Opin. Solid State Mater. Sci.* **10**, 61 (2006).
 - [13] C. Peter and K. Kremer, *Soft Matter* **5**, 4357 (2009).
 - [14] Y. Li, B. C. Abberton, M. Kröger, and W. K. Liu, *Polymers* **5**, 751 (2013).
 - [15] J. Padding and W. Briels, *J. Chem. Phys.* **117**, 925 (2002).
 - [16] L. Liu, J. Padding, W. den Otter, and W. Briels, *J. Chem. Phys.* **138**, 244912 (2013).
 - [17] K. M. Salerno, A. Agrawal, D. Perahia, and G. S. Grest, *Phys. Rev. Lett.* **116**, 058302 (2016).
 - [18] R. Faller and F. Müller-Plathe, *Polymer* **43**, 621 (2002).
 - [19] R. Faller and D. Reith, *Macromolecules* **36**, 5406 (2003).
 - [20] Y. Li, M. Kröger, and W. K. Liu, *Polymer* **52**, 5867 (2011).
 - [21] G. Maurel, F. Goujon, B. Schnell, and P. Malfreyt, *RSC Adv.* **5**, 14065 (2015).
 - [22] V. Harmandaris, N. Adhikari, N. F. van der Vegt, and K. Kremer, *Macromolecules* **39**, 6708 (2006).
 - [23] X. Chen, P. Carbone, W. L. Cavalcanti, G. Milano, and F. Müller-Plathe, *Macromolecules* **40**, 8087 (2007).
 - [24] D. Fritz, K. Koschke, V. A. Harmandaris, N. F. van der Vegt, and K. Kremer, *Phys. Chem. Chem. Phys.* **13**, 10412 (2011).
 - [25] H. A. Karimi-Varzaneh, P. Carbone, and F. Müller-Plathe, *J. Chem. Phys.* **129**, 154904 (2008).
 - [26] H. Eslami, H. A. Karimi-Varzaneh, and F. Müller-Plathe, *Macromolecules* **44**, 3117 (2011).
 - [27] C. Chen, P. Depa, J. K. Maranas, and V. G. Sakai, *J. Chem. Phys.* **128**, 124906 (2008).
 - [28] W. Tschöp, K. Kremer, J. Batoulis, T. Bürger, and O. Hahn, *Acta. Polym.* **49**, 61 (1998).
 - [29] C. F. Abrams and K. Kremer, *Macromolecules* **36**, 260 (2003).
 - [30] B. Hess, S. León, N. Van Der Vegt, and K. Kremer, *Soft Matter* **2**, 409 (2006).
 - [31] T. Strauch, L. Yelash, and W. Paul, *Phys. Chem. Chem. Phys.* **11**, 1942 (2009).
 - [32] G. Milano and F. Müller-Plathe, *J. Phys. Chem. B.* **109**, 18609 (2005).
 - [33] J. Baschnagel, K. Binder, P. Doruker, A. A. Gusev, O. Hahn, K. Kremer, W. L. Mattice, F. Müller-Plathe, M. Murat, and W. Paul, in *Viscoelasticity, atomistic models, statistical chemistry* (Springer, 2000), p. 41.
 - [34] P. Carbone, H. A. K. Varzaneh, X. Chen, and F. Müller-Plathe, *J. Chem. Phys.* **128**, 064904 (2008).
 - [35] M. E. Johnson, T. Head-Gordon, and A. A. Louis, *J. Chem. Phys.* **126**, 144509 (2007).
 - [36] S. K. Sukumaran, G. S. Grest, K. Kremer, and R. Everaers, *J. Polym. Sci., Part B: Polym. Phys.* **43**, 917 (2005).
 - [37] W. W. Graessley, *Adv. Polym. Sci.* **47**, 67 (1982).
 - [38] G. Marrucci, *J. Polym. Sci., Polym. Phys. Ed.* **23**, 159 (1985).
 - [39] M. Rubinstein and R. H. Colby, *J. Chem. Phys.* **89**, 5291 (1988).
 - [40] G. Marrucci and G. Ianniruberto, *Phil. Trans. R. Soc. Lond. A* **361**, 677 (2003).
 - [41] G. Ianniruberto and G. Marrucci, *J. Rheol.* **58**, 89 (2014).
 - [42] J. P. Wittmer, H. Meyer, J. Baschnagel, A. Johner, S. Obukhov, L. Mattioni, M. Müller, and A. N. Semenov, *Phys. Rev. Lett.* **93**, 147801 (2004).
 - [43] J. D. Halverson, W. B. Lee, G. S. Grest, A. Y. Grosberg, and K. Kremer, *J. Chem. Phys.* **134**, 204904 (2011).
 - [44] J. D. Halverson, G. S. Grest, A. Y. Grosberg, and K. Kremer, *Phys. Rev. Lett.* **108**, 038301 (2012).
 - [45] G. S. Grest, K. Kremer, S. T. Milner, and T. A. Witten, *Macromolecules* **22**, 1904 (1989).
 - [46] G. S. Grest and K. Kremer, *Macromolecules* **23**, 4994 (1990).
 - [47] E. R. Duering, K. Kremer, and G. S. Grest, *Phys. Rev. Lett.* **67**, 3531 (1991).
 - [48] C. Svaneborg, G. S. Grest, and R. Everaers, *Phys. Rev. Lett.* **93**, 257801 (2004).
 - [49] C. Svaneborg, R. Everaers, G. S. Grest, and J. G. Curro, *Macromolecules* **41**, 4920 (2008).
 - [50] T. Aoyagi, J.-I. Takimoto, and M. Doi, *J. Chem. Phys.* **115**, 552 (2001).
 - [51] F. Pierce, D. Perahia, and G. S. Grest, *Macromolecules* **42**, 7969 (2009).
 - [52] M. Murat and G. S. Grest, *Macromolecules* **24**, 704 (1991).
 - [53] M. Murat and G. S. Grest, *Phys. Rev. Lett.* **63**, 1074 (1989).
 - [54] G. S. Grest, *Phys. Rev. Lett.* **76**, 4979 (1996).
 - [55] H. Yagyu and T. Utsumi, *Comput. Mater. Sci.* **46**, 286 (2009).
 - [56] D. M. Sussman, W.-S. Tung, K. I. Winey, K. S. Schweizer, and R. A. Riggleman, *Macromolecules* **47**, 6462 (2014).
 - [57] D. Gersappe, *Phys. Rev. Lett.* **89**, 058301 (2002).
 - [58] T. Ge, M. O. Robbins, D. Perahia, and G. S. Grest, *Phys. Rev. E* **90**, 012602 (2014).
 - [59] G. S. Grest and K. Kremer, *Phys. Rev. A* **33**, 3628 (1986).
 - [60] K. Kremer and G. S. Grest, *J. Chem. Phys.* **92**, 5057 (1990).
 - [61] R. Faller, A. Kolb, and F. Müller-Plathe, *Phys. Chem. Chem. Phys.* **1**, 2071 (1999).
 - [62] R. Faller, F. Müller-Plathe, and A. Heuer, *Macromolecules* **33**, 6602 (2000).
 - [63] R. Faller and F. Müller-Plathe, *Chem. Phys. Chem.* **2**, 180 (2001).
 - [64] C. Svaneborg and R. Everaers, *Structure and dynamics of Kremer-Grest bead-spring polymer melts with adjustable stiffness at and beyond the Kuhn scale. Manuscript submitted to Macromolecules.* (2018).
 - [65] M. Rubinstein and R. H. Colby, *Polymer physics* (Oxford University, New York, 2003).
 - [66] W. Kuhn, *Kolloid.* **1**, 2 (1934).
 - [67] O. Kratky and G. Porod, *Rec. Trav. Chim.* **1106**, 2211 (1949).
 - [68] Y. Ding and A. P. Sokolov, *Macromolecules* **39**, 3322 (2006).
 - [69] P. J. Flory, *Science* **188**, 1268 (1975).
 - [70] L. J. Fetters, D. J. Lohse, and R. H. Colby, in *Physical properties of polymers handbook*, edited by J. Mark (Springer, 2007), p. 447.
 - [71] Y.-H. Lin, *Macromolecules* **20**, 3080 (1987).

- [72] T. A. Kavassalis and J. Noolandi, *Phys. Rev. Lett.* **59**, 2674 (1987).
- [73] N. Uchida, G. S. Grest, and R. Everaers, *J. Chem. Phys.* **128**, 044902 (2008).
- [74] M. Kröger, *Phys. Rep.* **390**, 453 (2004).
- [75] M. Abdel-Goad, W. Pyckhout-Hintzen, S. Kahle, J. Allgaier, D. Richter, and L. J. Fetters, *Macromolecules* **37**, 8135 (2004).
- [76] F. Vaca Chávez and K. Saalwächter, *Macromolecules* **44**, 1549 (2011).
- [77] D. Auhl, J. Ramirez, A. E. Likhtman, P. Chambon, and C. Fernyhough, *J. Rheol.* **52**, 801 (2008).
- [78] J. van Meerveld, *Rheol. Acta.* **43**, 615 (2004).
- [79] K. L. Ngai and D. J. Plazek, in *Physical Properties of Polymers Handbook* (Springer, 2007), p. 455.
- [80] A. E. Likhtman and T. C. McLeish, *Macromolecules* **35**, 6332 (2002).
- [81] K. Niedzwiedz, A. Wischniewski, W. Pyckhout-Hintzen, J. Allgaier, D. Richter, and A. Faraone, *Macromolecules* **41**, 4866 (2008).
- [82] J. Ramos, J. F. Vega, D. N. Theodorou, and J. Martinez-Salazar, *Macromolecules* **41**, 2959 (2008).
- [83] J.-X. Hou, C. Svaneborg, R. Everaers, and G. S. Grest, *Phys. Rev. Lett.* **105**, 068301 (2010).
- [84] R. B. Bird, R. C. Armstrong, and O. Hassager, *Dynamics of Polymeric Liquids*, vol. 1 (Wiley, New York, 1977).
- [85] H. Watanabe, *Prog. Polym. Sci.* **24**, 1253 (1999).
- [86] T. C. B. McLeish, *Adv. Phys.* **5**, 1379 (2002).
- [87] D. Richter, M. Monkenbusch, A. Arbe, and J. Colmenero, *Neutron spin echo in polymer systems* (Springer, 2005).
- [88] K. Saalwächter, *Prog. Nucl. Magn. Reson. Spectrosc.* **51**, 1 (2007).
- [89] A. Arbe, M. Monkenbusch, J. Stellbrink, D. Richter, B. Farago, K. Almdal, and R. Faust, *Macromolecules* **34**, 1281 (2001).
- [90] M. L. Williams, R. F. Landel, and J. D. Ferry, *J. Am. Chem. Soc.* **77**, 3701 (1955).
- [91] A. R. Khokhlov, A. Y. Grosberg, and V. S. Pande, *Statistical Physics of Macromolecules* (AIP-Press, Jericho NY, 1994).
- [92] P. E. Rouse, *J. Chem. Phys.* **21**, 1272 (1953).
- [93] F. Schmid, *J. Phys. Cond. Matter* **10**, 8105 (1998).
- [94] M. Müller and F. Schmid, in *Advanced Computer Simulation Approaches for Soft Matter Sciences II* (Springer, 2005), p. 1.
- [95] S. F. Edwards, *Proc. Phys. Soc.* **91**, 513 (1967).
- [96] P. G. de Gennes, *J. Chem. Phys.* **55**, 572 (1971).
- [97] S. F. Edwards, *Proc. Phys. Soc.* **92**, 9 (1967).
- [98] L. J. Fetters, D. J. Lohse, and W. W. Graessley, *J. Polym. Sci., Part B: Polym. Phys.* **37**, 1023 (1999).
- [99] L. J. Fetters, D. J. Lohse, S. T. Milner, and W. W. Graessley, *Macromolecules* **32**, 6847 (1999).
- [100] L. J. Fetters, D. J. Lohse, D. Richter, T. A. Witten, and A. Zirkel, *Macromolecules* **27**, 4639 (1994).
- [101] A. Rosa and R. Everaers, *Phys. Rev. Lett.* **112**, 118302 (2014).
- [102] H. J. Unidad, M. A. Goad, A. R. Bras, M. Zamponi, R. Faust, J. Allgaier, W. Pyckhout-Hintzen, A. Wischniewski, D. Richter, and L. J. Fetters, *Macromolecules* **48**, 6638 (2015).
- [103] A. Likhtman and T. McLeish, *Macromolecules* **35**, 6332 (2002).
- [104] G. Ianniruberto, A. Brasiello, and G. Marrucci, *Macromolecules* **45**, 8058 (2012).
- [105] S. L. Wingstrand, N. J. Alvarez, Q. Huang, and O. Hassager, *Phys. Rev. Lett.* **115**, 078302 (2015).
- [106] K. Z. Takahashi, R. Nishimura, N. Yamato, K. Yasuoka, and Y. Masubuchi, *Nature* **7**, 12379 (2017).
- [107] G. Zhang, T. Stuehn, K. C. Daoulas, and K. Kremer, *J. Chem. Phys.* **142**, 221102 (2015).
- [108] L. A. Moreira, G. Zhang, F. Müller, T. Stuehn, and K. Kremer, *Macromol. Theory Simul.* **24**, 419 (2015).
- [109] C. Svaneborg, H. A. Karimi-Varzaneh, N. Hojdis, F. Fleck, and R. Everaers, *Phys. Rev. E* **94**, 032502 (2016).
- [110] T. W. Sirk, Y. R. Slizoberg, J. K. Brennan, M. Lisal, and J. W. Andzelm, *J. Chem. Phys.* **136**, 134903 (2012).
- [111] I. Carmesin and K. Kremer, *Macromolecules* **21**, 2819 (1988).
- [112] S. Plimpton, *J. Comput. Phys.* **117**, 1 (1995).